arXiv:hep-ph/0411164v2 7 Dec 2005

Chaotic dynamics in preheating after inflation

Yoshida Jin[1,*] and Shinji Tsujikawa[2,†]
[1] *Department of Physics, Waseda University, Okubo 3-4-1, Shinjuku, Tokyo 169-8555, Japan*
[2] *Department of Physics, Gunma National College of Technology, Gunma 371-8530, Japan*
(Dated: February 2, 2008)

We study chaotic dynamics in preheating after inflation in which an inflaton ϕ is coupled to another scalar field χ through an interaction $(1/2)g^2\phi^2\chi^2$. We first estimate the size of the quasi-homogeneous field χ at the beginning of reheating for large-field inflaton potentials $V(\phi) = V_0\phi^n$ by evaluating the amplitude of the χ fluctuations on scales larger than the Hubble radius at the end of inflation. Parametric excitations of the field χ during preheating can give rise to chaos between two dynamical scalar fields. For the quartic potential ($n = 4$, $V_0 = \lambda/4$) chaos actually occurs for $g^2/\lambda < \mathcal{O}(10)$ in a linear regime before which the backreaction of created particles becomes important. This analysis is supported by several different criteria for the existence of chaos. For the quadratic potential ($n = 2$) the signature of chaos is not found by the time at which the backreaction begins to work, similar to the case of the quartic potential with $g^2/\lambda \gg 1$.

PACS numbers: 98.80.Cq

I. INTRODUCTION

Reheating after inflation is an extremely important stage to generate elementary particles present in current universe. In the original version of the reheating scenario which is now called *old reheating*, the decay of an inflaton field is characterized by a perturbative Born process [1]. However this process is not efficient for the success of the GUT-scale baryogenesis scenario. Later it was found that the existence of a nonperturbative stage– dubbed *preheating*– can lead to an explosive particle production prior to the Born decay [2, 3, 4].

During preheating scalar particles χ coupled to the inflaton ϕ are efficiently generated by parametric resonance through an interaction $(1/2)g^2\phi^2\chi^2$. The existence of the preheating stage provides several interesting possibilities such as the GUT-scale baryogenesis [5], nonthermal phase transition [6], the enhancement of metric perturbations [7] and the formation of primordial black holes [8]. In the chaotic inflationary scenario characterized by the potential $V(\phi) = V_0\phi^n$, the field perturbations $\delta\chi$ obey the Mathieu equation (for $n = 2$) or the Lame equation (for $n = 4$), which determines the structure of resonance at the linear regime. When the backreaction of created particles begins to violate the coherent oscillation of ϕ, this tends to work to suppress exponential growth of the field fluctuations. The system enters a fully nonlinear stage after which the mode-mode coupling (rescattering) between perturbations is crucially important [9, 10].

Typically the contribution of the dynamical background field χ is neglected in standard analysis of particle creations in preheating. This may be justified for a quadratic inflaton potential, since large-scale χ modes are exponentially suppressed during inflation for the coupling g required for preheating [11]. However the situation is different for a quartic inflaton potential with the coupling g of order $g^2/\lambda = \mathcal{O}(1)$ [12, 13]. In this case the quasi-homogeneous field χ can play an important role for the dynamics of preheating. In fact Podolsky and Starobinsky [14] pointed out that chaos may occur for the self-coupling potential $V(\phi) = (1/4)\lambda\phi^4$ when the coupling g^2/λ is not too much larger than of order unity. Since it is not obvious whether chaos actually occurs or not in this model only by analytic estimations, we shall perform detailed numerical investigation with/without the backreaction effect of created particles. We shall estimate the size of the field χ at the beginning of reheating by evaluating the amplitude of the χ fluctuations for the modes larger than the Hubble radius. To judge the existence of chaos in preheating we will adopt several different methods– such as the Toda-Brumer test [15, 16], Lyapunov exponents [17] and a fractal map [18].

It was already found that chaos appears for hybrid-type inflation models [19, 20, 21, 22] (see also Refs. [23, 24, 25]). Hybrid inflation is a rather special model in a sense that the symmetry breaking field automatically grows by tachyonic instability even if it is suppressed during inflation. The necessary condition for chaos is that there exist at least two dynamical fields and neither of them is too much smaller than another field. The hybrid model satisfies this condition, since two fields can have frequencies which are the same order after symmetry breaking. The presence of mixing terms between two fields leads to a new instability of perturbations in addition to tachyonic/resonance instabilities [21]. This new type of instability is clearly associated with the presence of chaos.

In this work we shall investigate the existence of chaos for large-field potentials $V(\phi) = V_0\phi^n$ with an interaction $(1/2)g^2\phi^2\chi^2$. We estimate the variance of large-scale modes in χ at the end of inflation, which is relevant to the initial condition of the quasi-homogeneous field χ for preheating. The field χ is amplified by parametric reso-

---

[*] Electronic address: jin@gravity.phys.waseda.ac.jp
[†] Electronic address: shinji@nat.gunma-ct.ac.jp

nance, which can give rise to chaos after χ grows to satisfy the Toda-Brumer condition. We shall numerically solve background equations together with perturbed equations for both quartic ($n = 4$) and quadratic ($n = 2$) potentials. Our main interest is to find the signature of chaos and the parameter range of the coupling g in which chaos can be seen before the backreaction effect of created particles becomes important. Since chaos can alter the standard picture of preheating by parametric resonance, it is of interest to clarify the situation in which chaos appears.

Recent observations suggest that the quartic potential $V(\phi) = (1/4)\lambda\phi^4$ is under an observational pressure, while the quadratic potential $V(\phi) = (1/2)m^2\phi^2$ is allowed [26]. This depends on the number of e-folds N before the end of inflation at which observable perturbations are generated. In the case of quartic potential this corresponds to $N \sim 64$ by assuming instant transitions between several cosmological epochs [27]. The likelihood analysis including WMAP and SDSS datasets shows that the quartic potential is marginally allowed by using $N = 64$ [28]. Therefore it is premature to rule out this model completely from current observations. The quartic potential corresponds to a system in which the background equations can be reduced to the ones in Minkowski spacetime by introducing conformal variables. This has an advantage for the investigation of chaotic dynamics during preheating. As we see later, the quartic potential exhibits a stronger chaos compared to the one for the quadratic potential.

II. THE FIELD VARIANCE FOR LONG WAVELENGTH MODES

In this section we shall estimate the field variance for long wavelength modes of the field χ coupled to the inflaton ϕ through an interaction $(1/2)g^2\phi^2\chi^2$. The effective potential in our system is

$$V(\phi,\chi) = V_0\phi^n + \frac{1}{2}g^2\phi^2\chi^2 \,. \tag{1}$$

We are mainly interested in two inflaton potentials: (i) the quadratic one ($n = 2$) and (ii) the quartic one ($n = 4$). In this work we do not implement nonminimal couplings [29] between the field χ and the scalar curvature R.

In a flat Friedmann-Lemaitre-Robertson-Walker (FLRW) background with a scale factor a, the background equations for the system (1) are

$$\ddot{\phi} + 3H\dot{\phi} + V_\phi = 0 \,, \tag{2}$$

$$\ddot{\chi} + 3H\dot{\chi} + V_\chi = 0 \,, \tag{3}$$

$$H^2 \equiv \left(\frac{\dot{a}}{a}\right)^2 = \frac{\kappa^2}{3}\left[\frac{1}{2}\dot{\phi}^2 + \frac{1}{2}\dot{\chi}^2 + V(\phi,\chi)\right] \,, \tag{4}$$

where $V_\phi = nV_0\phi^{n-1} + g^2\chi^2\phi$, $V_\chi = g^2\phi^2\chi$ and $\kappa^2 = 8\pi/m_p^2$ with m_p being the Planck mass.

We define the number of e-folds before the end of inflation, as

$$N \equiv \ln\left(a_f/a(t)\right) \,, \tag{5}$$

where a_f is the scale factor at the end of inflation. Employing the slow-roll approximation, $|\ddot{\phi}| \ll |3H\dot{\phi}|$ and $\dot{\phi}^2 \ll V(\phi)$, we easily find that $\mathrm{d}\phi/\mathrm{d}N = n/(\kappa^2\phi)$. Here we neglect the contribution coming from the χ-dependent terms. Integrating this equation, we obtain

$$\phi^2 - \phi_f^2 = \frac{2n}{\kappa^2}N \,. \tag{6}$$

The field value at the end of inflation (ϕ_f) is determined by setting the slow-roll parameter, $\epsilon_s \equiv (1/2\kappa^2)(V_\phi/V)^2$, is unity. This gives $\phi_f/m_p = n/(4\sqrt{\pi})$, thereby leading to

$$\phi^2 = \frac{n}{4\pi}\left(N + \frac{n}{4}\right)m_p^2 \,. \tag{7}$$

Let us consider a perturbation $\delta\chi$ in the field χ. Then the momentum-space first-order perturbed equation is given by

$$\delta\ddot{\chi}_k + 3H\delta\dot{\chi}_k + \left(\frac{k^2}{a^2} + g^2\phi^2\right)\delta\chi_k = 0 \,, \tag{8}$$

where k is a comoving wavenumber. Note that we neglected the backreaction of gravitational perturbations. When the effective mass of the field χ is larger than of order the Hubble rate, i.e., $g^2\phi^2 > (3H/2)^2$, the evolution of super-Hubble perturbations is characterized by underdamped oscillations with the dependence [11]

$$\delta\chi_k \propto a^{-3/2} \,. \tag{9}$$

Hence large-scale perturbations are exponentially suppressed during inflation. Meanwhile when $g^2\phi^2 < (3H/2)^2$ super-Hubble perturbations evolve as

$$\delta\chi_k \propto \exp\left[-\left(\frac{3}{2}H - \sqrt{\frac{9}{4}H^2 - g^2\phi^2}\right)\mathrm{d}t\right] \,. \tag{10}$$

This shows that in the massless limit ($g^2\phi^2 \ll H^2$) the amplitude of $\delta\chi_k$ decreases very slowly. In what follows we shall consider the quadratic and quartic models separately.

A. Quadratic model

For the inflation potential $V(\phi) = \frac{1}{2}m^2\phi^2$, the coupling g is required to be greater than of order 10^{-4} in order for preheating to occur [10]. In this case the resonance parameter, $q \equiv g^2\phi^2/(4m^2)$, is much larger than 1 at the beginning of preheating [10]. Since $H \sim m$ at the end of inflation, the existence of the preheating stage demands the condition $g^2\phi^2 \gg H^2$ during inflation. Hence the evolution of large-scale χ fluctuations is characterized by Eq. (9).

Let us consider the modes which are outside the Hubble radius at the end of inflation ($0 < k < k_f = a_f H_f$). Since these modes are effectively massive with slowly changing mass, they can be treated as an adiabatic state characterized by $\delta\chi_k = 1/(a^{3/2}\sqrt{2\omega_k})$ where $\omega_k^2 \simeq g^2\phi^2$. Hence the amplitude $|\delta\chi_k|^2$ at the end of inflation is estimated as

$$|\delta\chi_k(t_f)|^2 = \frac{1}{2a_f^3 g\phi_f}\,. \tag{11}$$

Then we can obtain the variance of the fluctuation $\delta\chi_k$ for $k < k_f$:

$$\begin{aligned}\langle\delta\chi_k^2(t_f)\rangle_{k<k_f} &= \frac{1}{2\pi^2}\int_0^{k_f} k^2|\delta\chi_k(t_f)|^2 \mathrm{d}k \\ &= \frac{\phi_f^2}{9\pi g}\sqrt{\frac{4\pi}{3}}\left(\frac{m}{m_p}\right)^3 \\ &= \frac{1}{9\pi\sqrt{12\pi}g}\left(\frac{m}{m_p}\right)^3 m_p^2\,, \end{aligned} \tag{12}$$

where we used $\phi_f = m_p/(2\sqrt{\pi})$ in addition to the slow-roll approximation $H^2 \simeq 4\pi m^2\phi^2/3m_p^2$.

For the quadratic potential ($n = 2$) the inflaton mass is constrained to be $m \simeq 10^{-6}m_p$ from the COBE normalization [30]. Then Eq. (12) shows that the variance is the function of g only. In Fig. 1 we plot $\sqrt{\langle\delta\chi_k^2(t_f)\rangle_{k<k_f}}$ as a function of g. It can be regarded as a quasi-homogeneous mode at the beginning of preheating. This at least measures the minimum amplitude of the homogeneous χ field.

B. Quartic model

For the quartic potential $V(\phi) = (1/4)\lambda\phi^4$, it is known that preheating occurs even when the coupling g is in the range $g^2\phi^2 \lesssim H^2$ [31, 32]. When $g^2/\lambda = \mathcal{O}(1)$, for example, the background dynamics transits from the "massless regime" [$g^2\phi^2 < (3H/2)^2$] to the "massive regime" [$g^2\phi^2 > (3H/2)^2$] during inflation [12, 13, 33]. The critical number of e-folds, N_c, in which the the evolution of the perturbation $\delta\chi_k$ transits from Eq. (10) to Eq. (9) is determined by the condition $9H_c^2/4 = g^2\phi_c^2$, which gives [33]

$$N_c = \frac{2}{3}\frac{g^2}{\lambda} = \ln\left(\frac{a_f}{a_c}\right) \simeq \ln\left(\frac{k_f}{k_c}\right)\,. \tag{13}$$

We note that we used the slow-roll condition

$$H^2 \simeq \frac{2\pi\lambda\phi^4}{3m_p^2}, \quad \phi^2 \simeq \frac{N}{\pi}m_p^2\,. \tag{14}$$

The modes which are inside the Hubble radius at transition time $t = t_c$ (but larger than the Hubble radius at the end of inflation) evolves as effective massive fields for $t > t_c$. Then for $k_c < k < k_f$ the amplitude $|\delta\chi_k|^2$ at the end of inflation is given by Eq. (11), which gives the variance

$$\begin{aligned}\langle\delta\chi_k^2(t_f)\rangle_{k_c<k<k_f} &= \frac{1}{2\pi^2}\int_{k_c}^{k_f} k^2|\delta\chi_k(t_f)|^2 \mathrm{d}k \\ &= \frac{\lambda}{18\pi^3}\sqrt{\frac{2\lambda}{3g^2}}(1-e^{-2g^2/\lambda})m_p^2\,, \end{aligned} \tag{15}$$

where we used the relation $k_c = k_f \exp(-2g^2/3\lambda)$ coming from Eq. (13).

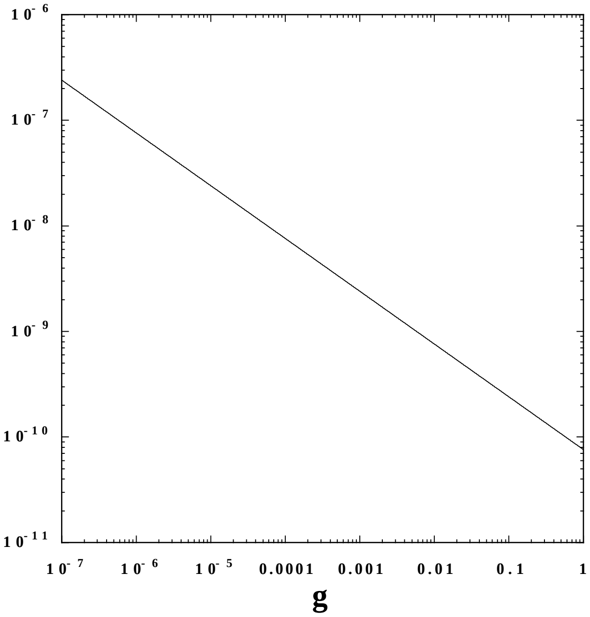

FIG. 1: The amplitude of the variance $\langle\delta\chi_k^2(t_f)\rangle_{k<k_f}^{1/2}$ at the end of inflation in terms of the function of the coupling g for the quadratic potential ($n = 2$). The variance gets smaller for larger g.

For $k < k_c$ the modes exit the Hubble radius before the transition time $t = t_c$. At the Hubble radius crossing ($t = t_k$) the amplitude of the perturbation $\delta\chi_k$ is given by

$$|\delta\chi_k(t_k)|^2 = \frac{H^2(t_k)}{2k^3}\,, \tag{16}$$

which comes from the quantization of a standard massless scalar field [30]. Since $\delta\chi_k$ evolve as Eq. (10) for $t_k < t < t_c$, we find that the amplitude of the perturbations at $t = t_c$ is given by [33]

$$|\delta\chi_k(t_f)|^2 = \frac{H^2(t_k)}{2k^3}e^{-3F(N_k)}\,, \tag{17}$$

where

$$F(N_k) \;=\; N_k - N_c - \sqrt{N_k(N_k-N_c)} \\ +N_c \ln\left(\frac{\sqrt{N_k}+\sqrt{N_k-N_c}}{\sqrt{N_c}}\right) . \qquad (18)$$

Here N_k is the number of e-folds at $t=t_k$. The perturbations evolve as Eq. (10) for $t_c < t < t_f$. Using Eq. (13) we obtain the following amplitude at the end of inflation:

$$|\delta\chi_k^2(t_f)| = \frac{H^2(t_k)}{2k^3} e^{-3F(N_k)-2g^2/\lambda} . \qquad (19)$$

Then the variance of perturbations $\delta\chi_k$ for the modes $k<k_c$ is given by

$$\begin{aligned} \langle\delta\chi_k^2(t_f)\rangle_{k<k_c} &= \frac{1}{2\pi^2}\int_{k_i}^{k_c} |\delta\chi_k(t_f)|^2 k^3 \mathrm{d}(\ln k) \\ &= \frac{1}{4\pi^2}\int_{N_c}^{N_i} \mathrm{d}N_k H^2(t_k) e^{-3F(N_k)-2g^2/\lambda} , \\ &= \frac{\lambda m_p^2}{6\pi^3}\int_{N_c}^{N_i} \mathrm{d}N_k N_k^2 e^{-3F(N_k)-2g^2/\lambda} , \end{aligned} \qquad (20)$$

where we used Eq. (14) and $\mathrm{d}(\ln k) \simeq \mathrm{d}(\ln a) = -\mathrm{d}N_k$. Note that k_i is the minimum wavenumber relevant for the maximum scale of cosmological perturbations. In order to obtain $\langle\delta\chi_k^2(t_f)\rangle_{k<k_c}$, it is necessary to solve the following differential equation:

$$\frac{\mathrm{d}}{\mathrm{d}N_k}\langle\delta\chi_k^2(t_f)\rangle_{k<k_c} = \frac{\lambda m_p^2}{6\pi^3} N_k^2 e^{-3F(N_k)-2g^2/\lambda}, \qquad (21)$$

which should be integrated from $N_c = 2g^2/3\lambda$ to N_i. Note that N_i roughly corresponds to the total number of e-folds during inflation. At least we require the condition $N_i > 60$. We shall choose $N_i = 60, 100, 1000$ in order to see the sensitivity for the change of this number.

Finally the variance for the modes $k < k_f$ is given by the following sum:

$$\langle\delta\chi_k^2(t_f)\rangle_{k<k_f} = \langle\delta\chi_k^2(t_f)\rangle_{k_c<k<k_f} + \langle\delta\chi_k^2(t_f)\rangle_{k<k_c} . \qquad (22)$$

When $g^2/\lambda \lesssim \mathcal{O}(1)$ one has $N_c \lesssim \mathcal{O}(1)$. This shows that most of the contribution to the variance $\langle\delta\chi_k^2(t_f)\rangle_{k<k_f}$ comes from the modes $k<k_c$. Meanwhile when $g^2/\lambda \gg 1$, i.e., $N_c \gg 1$, the modes $k_c<k<k_f$ dominate the total variance. In Fig. 2 we plot $\sqrt{\langle\delta\chi_k^2(t_f)\rangle_{k<k_f}}$ as a function of g^2/λ for $N_i = 60, 100, 1000$ and $\lambda = 10^{-13}$. We find that the variance does not depend on the values N_i for $g^2/\lambda \gtrsim 3$, which reflects the fact that Eq. (15) is independent of N_i. The difference appears for $g^2/\lambda \lesssim 3$, because of the fact that $\langle\delta\chi_k^2(t_f)\rangle_{k<k_c}$ is dependent on the values N_i. We shall use the values $\langle\delta\chi_k^2(t_f)\rangle_{k<k_f}$ obtained for $N_i = 60$ as a minimum initial condition of the quasi-homogeneous χ field at the beginning of preheating.

We note that Podolsky and Starobinsky [14] estimated the size of the quasi-homogeneous χ field for $g^2/\lambda = \mathcal{O}(1)$ by using a Fokker Planck equation [34]. This equation is valid when the mass of the field χ is smaller than of order the Hubble rate [35, 36, 37], which corresponds to $g^2/\lambda \lesssim \mathcal{O}(1)$. We checked that our estimation of the variance shows good agreement with the one based on the Fokker Planck approach for $g^2/\lambda \lesssim \mathcal{O}(1)$. In the parameter regime $g^2/\lambda \gg 1$ the Fokker Planck equation is no longer valid. Hence we need to use our estimation given above in order to know the size of the quasi-homogeneous χ field at the end of inflation.

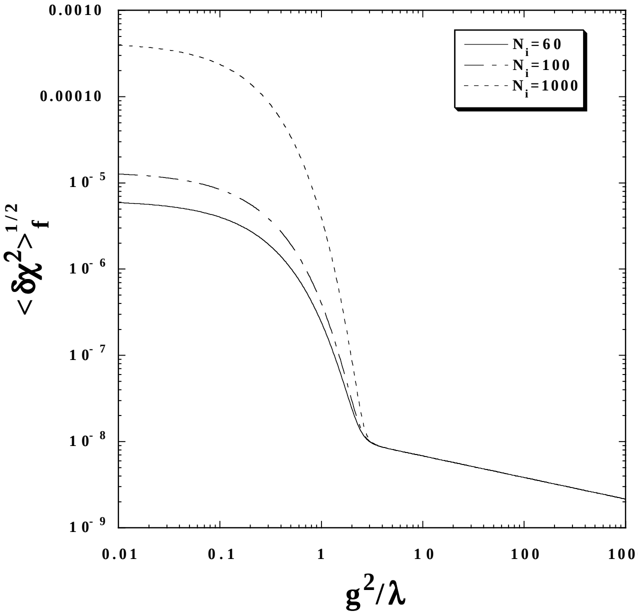

FIG. 2: The amplitude of the variance $\langle\delta\chi_k^2(t_f)\rangle_{k<k_f}^{1/2}$ at the end of inflation in terms of the function of the coupling g for the quartic potential ($n=4$). The variance is dominated by the modes $k_c<k<k_f$ for $g^2/\lambda \gg 1$, whereas the dominant contribution comes from the modes $k<k_c$ for $g^2/\lambda < \mathcal{O}(1)$.

III. BASIC PROPERTIES OF PREHEATING AND CHAOS

A. Preheating and the role of the quasi-homogeneous field χ

In the presence of the coupling $(1/2)g^2\phi^2\chi^2$, the coherent oscillation of the inflaton leads to the excitation of the field χ during preheating through the resonance term $g^2\phi^2\chi$ in Eq. (3). For the quadratic potential ($n=2$) parametric resonance is efficient when the condition, $q = g^2\phi^2/(4m^2) \gg 1$, is satisfied. To be more precise the field χ grows for $g \gtrsim 3.0 \times 10^{-4}$ by overcoming the friction due to cosmic expansion [10]. In this model the growth of χ ends when the system enters a narrow resonance regime ($q \lesssim 1$) or the backreaction effect of created particles breaks the coherent oscillation of the field ϕ. For the quartic potential ($n = 4$) resonance bands exist for the parameter space characterized by $n(2n-1) < g^2/\lambda < n(2n+1)$, where $n = 1, 2, 3, ...$ [31, 32]. The center of the band, $g^2/\lambda = 2n^2$, corresponds to the largest Floquet index ($\mu_{\rm max} \simeq 0.28$).

If the field χ is strongly suppressed during inflation, this does not contribute to the background dynamics even if it is amplified during reheating[1]. As we see in Figs. 1 and 2, it is expected that χ does not dynamically become important during preheating for larger g. However, for the quartic potential, parametric resonance takes place even for $g^2/\lambda = \mathcal{O}(1)$, in which case the quasi-homogeneous χ field does not suffer from strong suppression during inflation. Then if the quasi-homogeneous field χ is amplified during preheating, this can contribute to the background dynamics.

In our model the equations for field perturbations in Fourier space may be written as [14]

$$\delta\ddot{\phi}_k + 3H\delta\dot{\phi}_k + \left[\frac{k^2}{a^2} + n(n-1)V_0\phi^{n-2} + g^2\chi^2\right]\delta\phi_k = -2g^2\phi\chi\delta\chi_k\,, \tag{23}$$

$$\delta\ddot{\chi}_k + 3H\delta\dot{\chi}_k + \left(\frac{k^2}{a^2} + g^2\phi^2\right)\delta\chi_k = -2g^2\phi\chi\delta\phi_k\,, \tag{24}$$

where k is a comoving wavenumber. This corresponds to the equations in which the contributions from metric perturbations are dropped (see Ref. [7]). Since metric perturbations are enhanced only when field fluctuations grow sufficiently, it is a good approximation to neglect them except for a nonlinear stage of preheating.

The terms on the r.h.s. of Eqs. (23) and (24) are not usually taken into account in standard analysis of preheating [2, 3, 10], since the field χ was supposed to be dynamically unimportant. However this can give considerable contributions to the dynamics of field perturbations provided that the quasi-homogeneous field χ is not strongly suppressed during inflation. In fact these terms lead to a mixing between the perturbations of two fields, whose behavior is absent in standard analysis of preheating unless rescattering effects are taken into account at a nonlinear stage.

We start integrating background and perturbation equations from the end of inflation. We adopt the Bunch-Davies vacuum state for the initial condition of perturbations for the modes inside the Hubble radius. The total variances of the fields $\varphi = \phi, \chi$ integrated in terms of k are

$$\langle\delta\varphi^2\rangle = \frac{1}{2\pi^2}\int k^2|\delta\varphi_k|^2{\rm d}k\,. \tag{25}$$

We implement the variances $\langle\delta\phi^2\rangle$ and $\langle\delta\chi^2\rangle$ for both background and perturbation equations as a Hartree approximation [10]. We note that this is for estimating the time at which backreaction effects become important. After the system enters a fully nonlinear stage, one can not trust the analysis using the Hartree approximation. Our interest is to find a signature of chaos before the backreaction sets in.

B. The condition for chaos

In this subsection we review several conditions for the existence of chaos and apply them to our effective potential (1). Let us consider the first-order differential equations

$$\dot{x}_i = F_i(x_j)\,, \tag{26}$$

and their linearized equations,

$$\delta\dot{x}_i = \frac{\partial F_i}{\partial x_j}\,\delta x_j\,, \tag{27}$$

where δx_i is the perturbation vector connecting two nearby trajectories and $\partial F_i/\partial x_j$ is the Jacobian matrix of $F_i(x_j)$.

The scalar-field equations (2) and (3) are expressed by the form (26) by setting $x_1 = \phi$, $x_2 = \dot{\phi}$, $x_3 = \chi$ and $x_4 = \dot{\chi}$. Then one can evaluate the Jacobian matrix $\partial F_i/\partial x_j$ and its eigenvalues μ for a general system characterized by an effective potential $V = V(\phi, \chi)$. Note that we do not account for the linearized equation for H, since metric perturbations are neglected in our analysis. The eigenvalues of the matrix $\partial F_i/\partial x_j$ are given by

$$\mu = \frac{1}{2}\left[-3H \pm \sqrt{9H^2 + 4\gamma}\right]\,, \tag{28}$$

where

$$\gamma = \frac{1}{2}\Big[-(V_{\phi\phi} + V_{\chi\chi}) \pm\sqrt{(V_{\phi\phi} + V_{\chi\chi})^2 - 4(V_{\phi\phi}V_{\chi\chi} - V_{\phi\chi}^2)}\Big]\,. \tag{29}$$

The necessary condition for the existence of chaos is that one of the eigenvalues is at least positive. In an expanding background ($H > 0$) this corresponds to the condition $\gamma > 0$ from Eq. (28). Since we are now considering a situation in which both effective masses of ϕ and χ are positive ($V_{\phi\phi} > 0$, $V_{\chi\chi} > 0$), γ can take a positive value when

$$V_{\phi\phi}V_{\chi\chi} - V_{\phi\chi}^2 < 0\,. \tag{30}$$

This is so-called the Toda-Brumer test [15, 16] that is used to judge the existence of chaos. For our effective potential (1) this translates into the condition

$$\chi^2 > \frac{n(n-1)V_0}{3g^2}\phi^{n-2}\,. \tag{31}$$

---

[1] The amplification of χ is limited by the backreaction effect of created particles.

When $n = 2$ and $V_0 = m^2/2$, this corresponds to

$$\chi > \frac{m}{\sqrt{3}g}\,, \tag{32}$$

whereas for $n = 4$ and $V_0 = \lambda/4$ we get

$$\chi > \sqrt{\frac{\lambda}{g^2}}\,\phi\,. \tag{33}$$

For the quadratic potential the initial value of χ is $10^{-4}\sqrt{g}$ times smaller than the value which leads to chaotic instability, see Eqs. (12) and (32). Therefore the system is expected to enter a chaotic phase after the field is amplified more than $10^4/\sqrt{g}$ times. For the quartic potential the condition for chaos is not so severe compared to the quadratic potential, since the term on the r.h.s. of Eq. (33) decreases with time.

It is worth commenting on the difference about the instabilities of chaos and parametric resonance. Although the field χ exhibits an exponential growth by resonance, this is different from the chaotic instability in which the evolution of the system is very sensitive to slight change of initial conditions. In fact none of the eigenvalues of the Jacobi matrix is positive in the regime where the condition (31) is not satisfied. This means that chaos is absent in the region $\chi^2 < n(n-1)V_0/(3g^2)\phi^{n-2}$ even if the field shows an exponential growth by parametric resonance.

Since the Toda-Brumer test is not a sufficient condition for the existence of chaos, we shall use other criteria as well such as Lyapunov exponents [17]. The Lyapunov exponents measure the logarithm of of the expansion of a small volume in a N-dimensional phase space. In this case the system possesses N Lyapunov exponents. Chaos is accompanied by an increase of the size of the N-volume at least in one direction and a maximal Lyapunov exponent h characterizes the signature of chaos. When h approaches a positive constant asymptotically, this shows the existence of chaos since the initial displacement of the N-volume grows exponentially. If h approaches to 0 asymptotically, this means the absence of chaos since the orbits are periodic or quasi-periodic. Strictly speaking Lyapunov exponents are defined in the limit $t \to \infty$. Nevertheless one can check the existence of chaos by investigating the behavior of the system for sufficiently large values of t. In fact, as we see later, the maximal Lyapunov exponent begins to grow toward a constant value when chaos appears. Although the backreaction effect of created particles can alter the background dynamics, it is possible to see the signature of chaos before the backreaction sets in.

In addition to the above two criteria, there exists another criterion for the existence of chaos– which is so called a fractal map [18]. This strategy is useful because of gauge independence which comes from using a topological character. In the next section we shall also use this criterion to confirm the presence of chaos in addition to other methods.

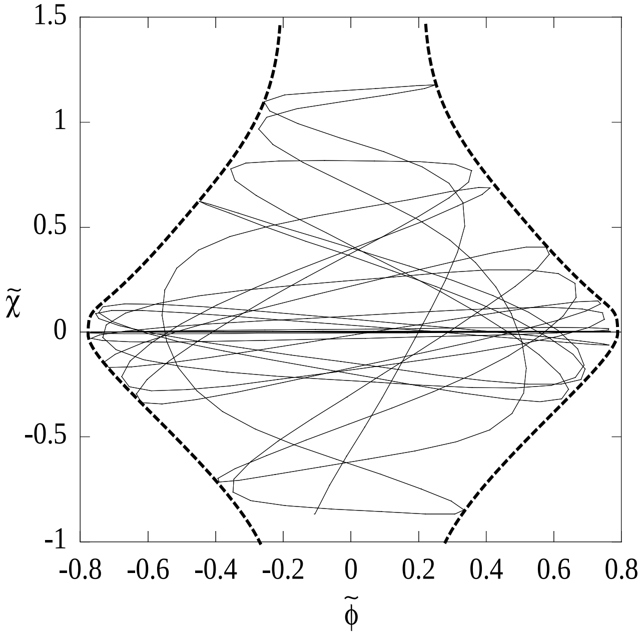

FIG. 3: A phase-space trajectory in the (ϕ, χ) plane for $g^2/\lambda = 2$. The dotted curve corresponds to the boundary given in Eq. (37).

IV. CHAOTIC DYNAMICS FOR THE QUARTIC POTENTIAL

For the quartic potential ($n = 4$) the system is effectively reduced to a Hamiltonian system in Minkowski spacetime by introducing conformal variables: $\tilde{\phi} \equiv a\phi$ $\tilde{\chi} \equiv a\chi$ and $\eta \equiv \int a^{-1}dt$. Using the fact that $a \propto \eta$ and a'/a, $a''/a \to 0$ during reheating in this model, the background equations (2), (3) and (4) can be written as

$$\tilde{\phi}'' + \lambda\tilde{\phi}^3 + g^2\tilde{\chi}^2\tilde{\phi} = 0\,, \tag{34}$$

$$\tilde{\chi}'' + g^2\tilde{\phi}^2\tilde{\chi} = 0, \tag{35}$$

$$\begin{aligned} a'^2 &= \frac{8\pi}{3m_p^2}\left(\frac{1}{2}\tilde{\phi}'^2 + \frac{1}{2}\tilde{\chi}'^2 + \frac{\lambda}{4}\tilde{\phi}^4 + \frac{g^2}{2}\tilde{\phi}^2\tilde{\chi}^2\right) \\ &\equiv \frac{8\pi}{3m_p^2}E = \text{const}\,, \end{aligned} \tag{36}$$

where a prime denotes the derivative with respect to conformal time η. The trajectories of the fields are bounded by

$$\frac{\lambda}{4}\tilde{\phi}^4 + \frac{g^2}{2}\tilde{\phi}^2\tilde{\chi}^2 \le E\,. \tag{37}$$

This boundary is plotted as a dotted curve in Fig. 3.

From the Toda-Brumer test (33), we can expect that chaos occurs when χ becomes comparable to ϕ for $g^2/\lambda = \mathcal{O}(1)$. When $1 < g^2/\lambda < 3$, corresponding to the first resonance band [31, 32], the variance of the field χ is larger than $\chi_f \sim 10^{-8}m_p$ right after the end of inflation from Fig. 2. We require the parametric excitation of χ to give

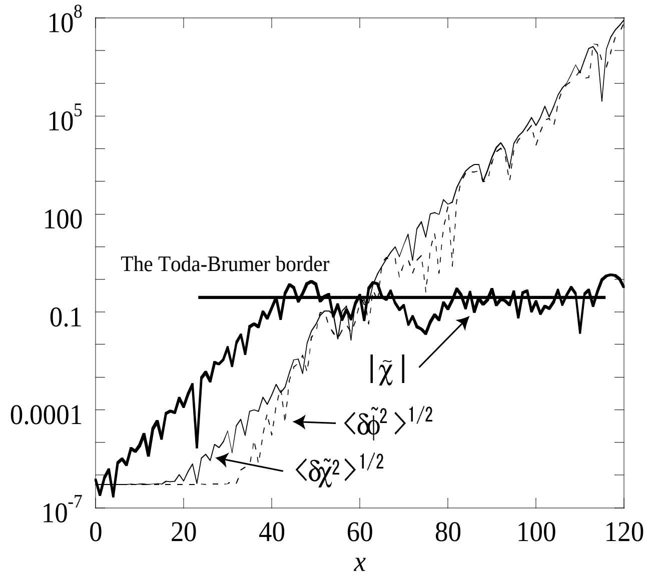

FIG. 4: Evolution of $\tilde{\chi}$, $\langle\delta\tilde{\chi}^2\rangle^{1/2}$ and $\langle\delta\tilde{\phi}^2\rangle^{1/2}$ (normalized by m_p) as a function of $x \equiv \sqrt{\lambda}\phi_I\eta$ for $g^2/\lambda = 2$ when the backreaction effect of created particles is neglected. The horizontal line shows the border of the Toda-Brumer test. The perturbations in ϕ and χ exhibit instabilities associated with chaos once the field χ is sufficiently amplified.

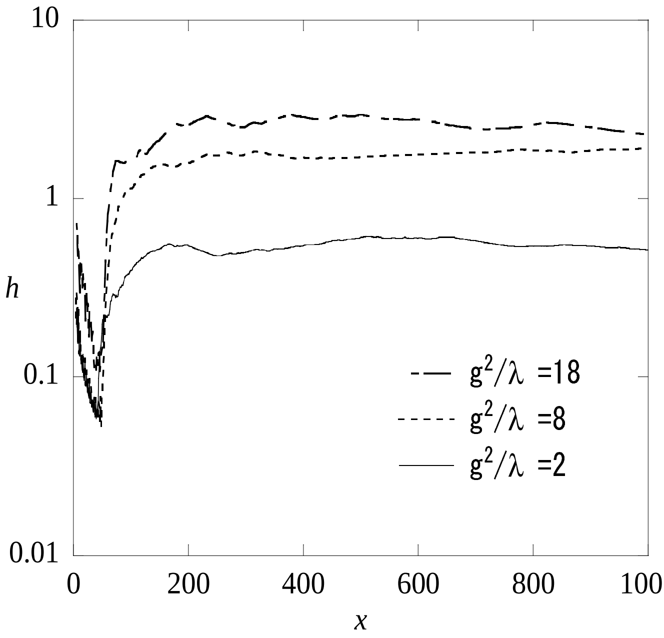

FIG. 5: Evolution of the maximal Lyapunov exponent h for $g^2/\lambda = 2, 8, 18$. We do not implement the backreaction effect of created particles. We find that the exponent h approaches a constant value in these cases.

rise to chaos, since χ is much smaller than ϕ at the beginning of reheating. Therefore the coupling g needs to lie inside of the resonance band for the existence of chaos. In Fig. 3 we show an example of the background trajectory for $g^2/\lambda = 2$. We find that two fields evolve chaotically in the phase-space of the (ϕ, χ) plane by choosing several different initial conditions.

When $g^2/\lambda = 2$ the Toda-Brumer test gives the condition $\tilde{\chi}/m_p \gtrsim 0.5$ for the existence of chaos, which corresponds to the time $x \equiv \sqrt{\lambda}\phi_I\eta \gtrsim 45$ (see Fig. 4). We find that the fluctuations $\langle\delta\tilde{\chi}^2\rangle$ and $\langle\delta\tilde{\phi}^2\rangle$ exhibit rapid increase with a similar growth rate after the field χ satisfies the Toda-Brumer test. It is expected that this is associated with the presence of chaos rather than parametric excitation of the χ fluctuation. The quasi-homogeneous field χ is amplified by parametric resonance for $x \lesssim 45$ but stops growing after that. This comes from the fact that the resonance does not occur once the homogeneous oscillation of ϕ is broken by the growth of χ. The $g^2\phi^2$ term on the l.h.s. of Eq. (24) also becomes ineffective at this stage, but the presence of the mixing term on the r.h.s. leads to a new type of instability associated with chaos. The rapid growth of $\langle\delta\tilde{\phi}^2\rangle$ seen in Fig. 4 also comes from the mixing term on the r.h.s. of Eq. (23) rather than from the parametric excitation of sub-Hubble modes with $3/2 < k^2/(\lambda\phi_I^2) < \sqrt{3}$ [31, 32].

In order to check the existence of chaos, we plot the evolution of the maximal Lyapunov exponent h for several different values of g in Fig. 5. The exponent decreases at the initial stage even though χ is amplified by parametric resonance. However h begins to grow after χ satisfies the Toda-Brumer test (33). The system eventually approaches a phase with a positive constant h, which shows the existence of chaos. The growth of the maximal Lyapunov exponent is regarded as a signature of chaos, since this behavior can not be seen in the absence of chaos. We checked that h continues to decrease and converges toward 0 in power if the mixing terms do not exist on the r.h.s. of Eqs. (23) and (24).

In Fig. 6 we show a fractal map for $g^2/\lambda = 2$ with slight change of initial conditions in terms of $\tilde{\chi}_I$ and $\tilde{\dot{\chi}}_I$. We set exit pockets when the field χ becomes larger than $|\tilde{\chi}| = 1.2$. When an orbit reaches a pocket we assign colors to many initial conditions as in the following way; white if an orbit falls down to an upper pocket ($\tilde{\chi} > 1.2$), black if it falls down to a lower pocket ($\tilde{\chi} < -1.2$). Figure 6 is the result of the above manipulation, which shows that the map of initial conditions is fractal. This means that orbits are sensitive to initial data, thereby showing the existence of chaos.

The above discussion neglects the backreaction effect of created particles. If we account for it as a Hartree approximation, Eqs. (2), (3), (4), (23) and (24) are modified by replacing the ϕ^2, χ^2 and ϕ^3 terms for $\phi^2 + \langle\delta\phi^2\rangle$, $\chi^2 + \langle\delta\chi^2\rangle$ and $\phi^3 + 3\phi\langle\delta\phi^2\rangle$, respectively [10]. By Eq. (23) the backreaction becomes important when

$$\sqrt{\langle\delta\tilde{\chi}^2\rangle} \gtrsim \sqrt{\frac{3\lambda}{g^2}}\,\tilde{\phi}\,. \qquad (38)$$

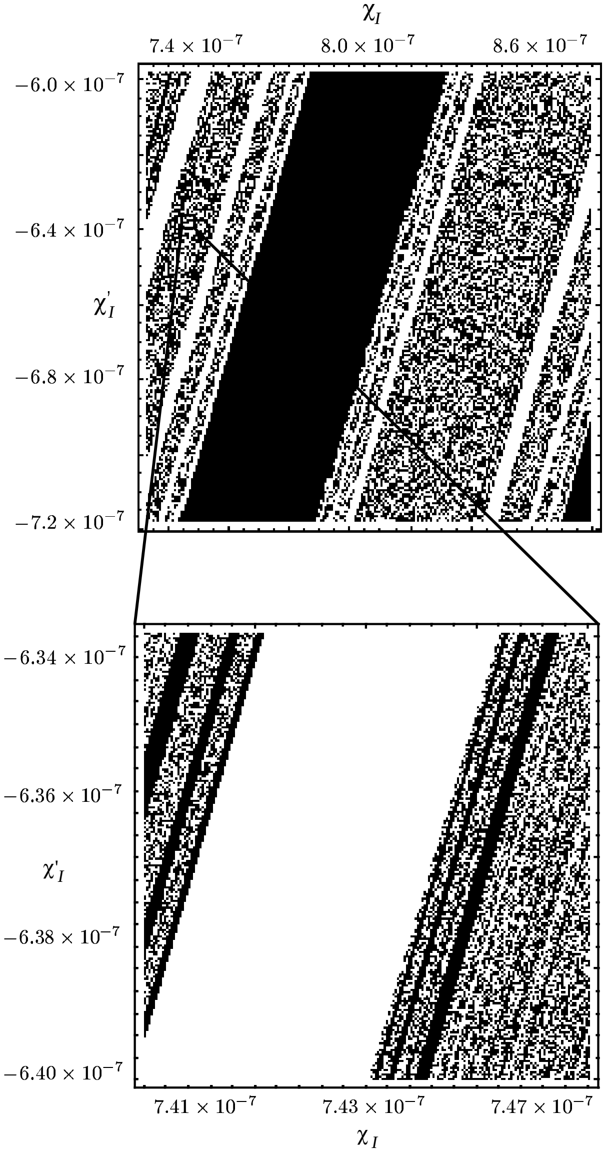

FIG. 6: A fractal map for $g^2/\lambda = 2$. We show the map of initial conditions χ_I and $\dot{\chi}_I$ with exit pockets characterized by $|\tilde{\chi}| \geq 1.2$. The white color corresponds to orbits which give $\tilde{\chi} \geq 1.2$, whereas the black one to orbits which give $\tilde{\chi} \leq -1.2$. The upper panel corresponds to the change of initial conditions by 0.1%. The lower panel is an extended figure, in which initial conditions change by 0.005%. These figures exhibit fractal structures, which result from sensitivity to initial conditions.

This is similar to the necessary condition for chaos for the background field χ, see Eq. (33). When $g^2/\lambda = \mathcal{O}(1)$, the Toda-Brumer test is satisfied before the condition (38) is fulfilled. As seen in Fig. 4 both $\tilde{\chi}^2$ and $\langle\delta\tilde{\chi}^2\rangle$ have similar amplitudes initially, but the growth of sub-Hubble fluctuations occurs later than that of $\tilde{\chi}^2$. At the time when the Toda-Brumer test (33) is satisfied ($x \simeq 45$), $\langle\delta\tilde{\chi}^2\rangle$ is much smaller than $\tilde{\chi}^2$ for $g^2/\lambda = 2$. The

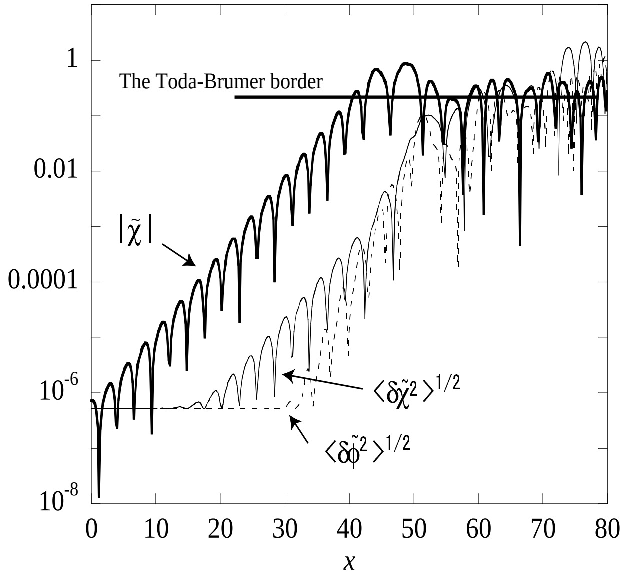

FIG. 7: Evolution of $\tilde{\chi}$, $\langle\delta\tilde{\chi}^2\rangle^{1/2}$ and $\langle\delta\tilde{\phi}^2\rangle^{1/2}$ (normalized by m_p) for $g^2/\lambda = 2$ when the backreaction effect is taken into account. The horizontal line corresponds to the Toda-Brumer border.

backreaction effect becomes important around $x = 60$ in this case.

By implementing the backreaction as a Hartree approximation, we find that this typically tends to work to suppress the growth of field fluctuations. As illustrated in Fig. 7 the fluctuations do not exhibit rapid growth after the backreaction begins to work ($x \gtrsim 60$). Nevertheless we need to caution that linear perturbation theory is no longer valid at this stage. For completeness it is required to account for the mode-mode coupling (rescattering) between the fluctuations [9]. In fact we found a numerical instability for $x \gtrsim 80$ in the simulation of Fig. 7, which signals the limitation of the Hartree approximation. It is of interest to see the effect of chaos at this fully nonlinear stage, but this is a non-trivial problem because of the complex nature of reheating. Note that the chaotic period ends at some time to complete reheating. It is difficult to judge when chaos ends in our system, since the mechanism for the decay of ϕ and χ after preheating is not completely known.

When $g^2/\lambda = \mathcal{O}(1)$ one can find out the existence of chaos during a short period before the backreaction begins to work. As we already mentioned, the criterion for chaos is given by Eq. (33), whereas the criterion for the backreaction corresponds to Eq. (38). The initial value of the quasi-homogeneous field χ gets smaller for larger g^2/λ, as illustrated in Fig. 2. This means that the condition (38) tends to be satisfied prior to the time at which the quasi-homogeneous field χ grows to satisfy the Toda-Brumer test (33). In Fig. 8 we plot the evolution of the system for $g^2/\lambda = 5000$ with the backreaction effect of created particles. In this case the backreaction becomes

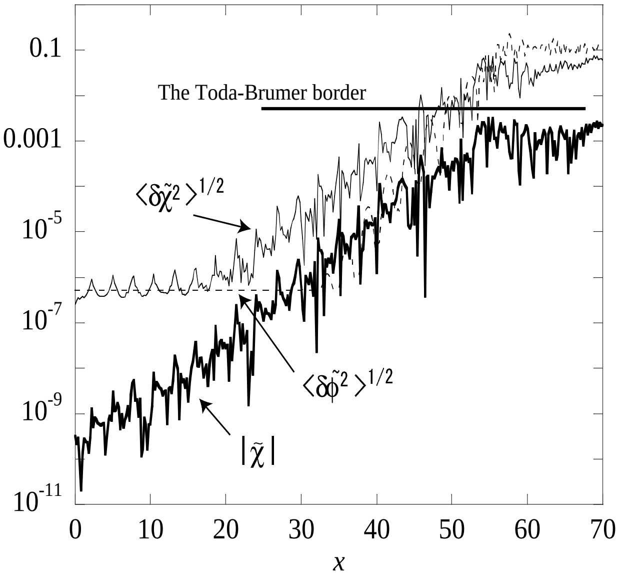

FIG. 8: As in Fig. 7 for $g^2/\lambda = 5000$.

important around $x = 50$ before the quasi-homogeneous field χ increases sufficiently to satisfy the Toda-Brumer test. Therefore, when $g^2/\lambda \gg 1$, we do not find a signature of chaos before the perturbations reach a nonlinear regime.

For the coupling g that belongs to the resonance bands $n(2n-1) < g^2/\lambda < n(2n+1)$, we find that chaos occurs for

$$g^2/\lambda < \mathcal{O}(10)\,, \tag{39}$$

before the backreaction begins to work. We note that this result is obtained by using the value $\sqrt{\langle \delta\chi_k^2(t_f)\rangle_{k<k_f}}$ derived in Sec. II as the initial condition of χ at the beginning of preheating. When $g^2/\lambda > \mathcal{O}(10)$ the field fluctuation $\langle\delta\tilde{\chi}^2\rangle$ satisfies the condition (38) prior to the time at which the necessary condition for chaos is fulfilled. Provided that $g^2/\lambda \gg 1$, the standard Floquet theory of parametric resonance [31, 32] is valid at the linear level, since the effect of the quasi-homogeneous field χ is not important relative to its perturbations on sub-Hubble scales.

V. QUADRATIC POTENTIAL

For the quadratic potential the system can not be reduced to the analysis in Minkowski spacetime by introducing conformal quantities. Therefore the analysis in the quadratic potential is more complicated than in the case of the quartic potential in an expanding background.

We start our analysis by studying the two-field dynamics in a frictionless background. In this case the fields oscillate coherently without an adiabatic damping due to cosmic expansion. The system has the field equations corresponding to $H = 0$ in Eqs. (2) and (3) together with the constraint

$$E = \frac{1}{2}\dot{\phi}^2 + \frac{1}{2}\dot{\chi}^2 + V(\phi,\chi)\,, \tag{40}$$

where E is conserved. Unlike the case of an expanding background, the field χ is enhanced only when the system is inside of resonance bands from the beginning of preheating. This comes from the fact that the field χ does not shift to other stability/instability bands in the absence of cosmic expansion [10]. We wish to study the existence of chaos for the coupling g that leads to parametric excitation of χ in an expanding background ($g \gtrsim 3.0\times10^{-4}$). First we carry out the analysis in a conserved Hamiltonian system given above and then proceed to the case in which the expansion of universe is taken into account.

As illustrated in Fig. 1, the quasi-homogeneous χ field at the end of inflation is estimated to be $\chi_f \lesssim 10^{-9}$-$10^{-8}m_p$ for the coupling $g \gtrsim 3.0\times10^{-4}$, which is smaller than that in the quartic potential with $g^2/\lambda = \mathcal{O}(1)$. Hence the field χ for the quadratic potential is more strongly suppressed during inflation for the values of g relevant to efficient preheating.

In Fig. 9 we plot the evolution of the background field χ together with $\sqrt{\langle\delta\chi^2\rangle}$ and $\sqrt{\langle\delta\phi^2\rangle}$ for the coupling $g = 3.0\times10^{-4}$. Note that we implement the backreaction of sub-Hubble field fluctuations as a Hartree approximation. In this case the Toda-Brumer test gives the condition $\chi/m_p > 1.9\times10^{-3}$ by Eq. (32). For the quadratic potential the backreaction begins to work for $\langle\delta\chi^2\rangle \gtrsim m^2/g^2$, which is basically a similar condition to the Toda-Brumer test for the background field χ. As shown in Fig. 9 the quasi-homogeneous field χ does not satisfy the Toda-Brumer test, since the backreaction becomes important before χ grows sufficiently.

The quasi-homogeneous χ field at the end of inflation gets smaller for larger g, see Eq. (12). Figure 10 shows the evolution of the system for $g = 3.0\times10^{-3}$, in which case the initial variance of the field χ is suppressed relative to the case $g = 3.0\times10^{-4}$. Although the condition for chaos using the Toda-Brumer test (32) gets milder for larger g, this property is compensated by the suppression of the quasi-homogeneous field χ at the beginning of preheating. Therefore it is difficult to satisfy the necessary condition for chaos before the backreaction begins to work. We carried out numerical simulations for other values of g and found that the signature of chaos is not seen in the frictionless system as long as the backreaction effect is taken into account.

If we implement the effect of cosmic expansion, the energy of the system given by Eq. (40) decreases. In fact the time-derivative of E is given by

$$\frac{\mathrm{d}E}{\mathrm{d}t} = -3H(\dot{\phi}^2 + \dot{\chi}^2) \simeq -3HE\,, \tag{41}$$

where we used the approximation $E \simeq \dot{\phi}^2 + \dot{\chi}^2$. Then the energy lost during one oscillation of the inflaton ($\Delta t \simeq$

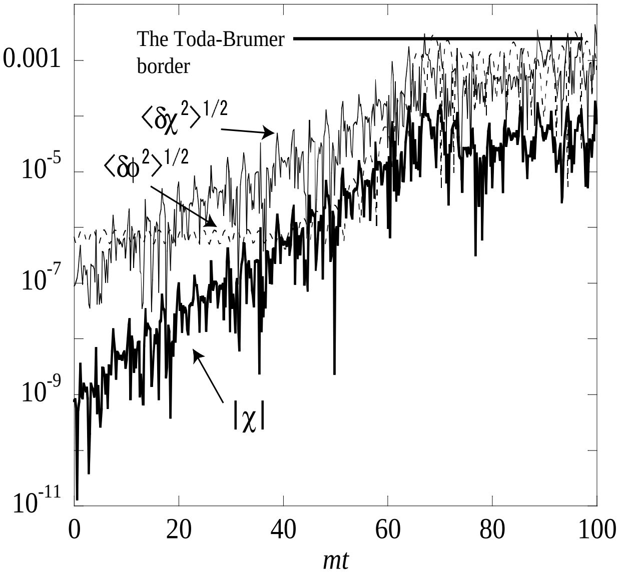

FIG. 9: Evolution of χ, $\langle\delta\chi^2\rangle^{1/2}$ and $\langle\delta\phi^2\rangle^{1/2}$ (normalized by m_p) for $g = 3.0\times10^{-4}$ without the friction due to cosmic expansion. The horizontal line represents the border of the Toda-Brumer test. We implement the backreaction effect of created particles as a Hartree approximation.

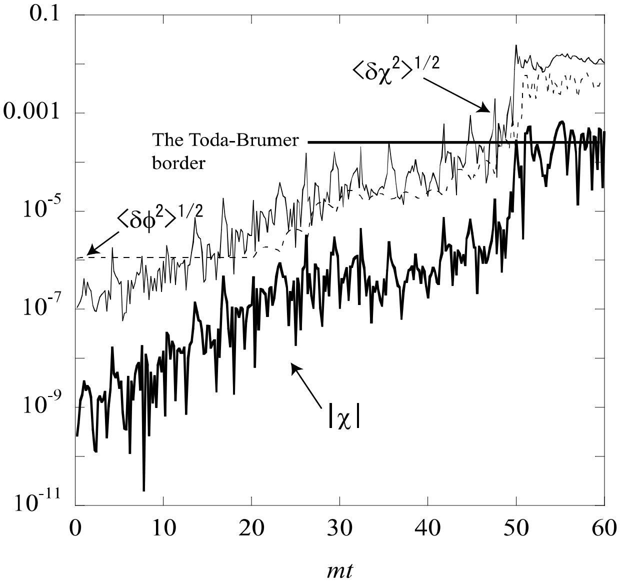

FIG. 10: As in Fig. 9 with $g = 3.0\times10^{-3}$.

$1/m$) is estimated as

$$\frac{\Delta E}{E} \simeq -3\frac{H}{m} \simeq -\sqrt{24\pi}\frac{\phi}{m_p}\,. \qquad (42)$$

Therefore the energy loss is large at the beginning of preheating ($|\Delta E/E| \gtrsim 0.1$), but it becomes smaller and smaller with time. The analysis in the frictionless system can be used in an expanding background when the condition, $|\Delta E/E| \ll 1$, is satisfied.

In addition to the energy loss, we need to caution that the structure of resonance changes in the presence of cosmic expansion. The field χ passes many instability/stability bands, which is generally called *stochastic resonance* [10]. Parametric resonance ends when the resonance parameter, $q = g^2\phi^2/(4m^2)$, drops down to less than of order unity, whose property is different from the analysis in Minkowski spacetime.

In spite of above complexities, it is possible to check whether the signature of chaos is seen or not in a linear perturbation regime. Note that the Toda-Brumer condition is valid in an expanding background. We run our numerical code including the backreaction of sub-Hubble field fluctuations for the coupling g relevant to efficient preheating ($g \gtrsim 3.0\times10^{-4}$) and find that the background χ stops growing by the backreaction effect before the Toda-Brumer condition is satisfied. This property is similar to the case discussed in the frictionless background. Therefore chaos does not appear for the quadratic potential at least in a regime before the backreaction sets in.

VI. CONCLUSIONS

In this paper we discussed chaotic dynamics in two-field preheating with monomial inflaton potentials $V(\phi) = V_0\phi^n$. A scalar field χ coupled to inflaton with an interaction $(1/2)g^2\phi^2\chi^2$ is amplified by parametric resonance when the inflaton oscillates coherently. As long as the background field χ is not strongly damped in an inflationary epoch, χ can grow to the same order as ϕ, thereby giving rise to a possibility of chaos during preheating.

First we estimated the amplitude of the quasi-homogeneous χ field at the beginning of reheating by considering the variance of the χ fluctuations on scales larger than the Hubble radius at the end of inflation. The variance $\sqrt{\langle\delta\chi_k^2(t_f)\rangle_{k<k_f}}$ is plotted as a function of the coupling g in Figs. 1 and 2. For the quartic inflaton potential with $g^2/\lambda = \mathcal{O}(1)$ there exist large-scale perturbation modes ($k < k_c$) which are not strongly suppressed during inflation. Then this gives large contribution to the total variance of χ relative to the case $g^2/\lambda \gg 1$ at the end of inflation.

Typically the background field χ is assumed to be negligible in standard analysis of particle creations in preheating, but its presence leads to a mixing between two fields. This gives rise to a chaotic instability in addition to the enhancement of perturbations by parametric resonance. We note that standard Floquet theory using Mathieu or Lame equation ceases to be valid when the chaos is present. This new channel of instability can alter the maximum size of field fluctuations if two dynamical fields do not decay for a long time.

In order to study whether chaos really appears or not, we solved the background equations (2), (3) and (4) together with perturbed equations (23) and (24). For a quartic potential ($n = 4$ and $V_0 = \lambda/4$) parametric resonance can occur for the coupling g^2/λ of order unity. In this case the quasi-homogeneous field χ satisfies the Toda-Brumer test (33) before the backreaction effect of created particles becomes important. Since this is only the necessary condition for chaos, we also evaluated Lyapunov exponents for $g^2/\lambda = \mathcal{O}(1)$ in order to confirm the presence of chaos. We find that the maximal Lyapunov exponent begins to increase toward a positive constant value after the Toda-Brumer condition is satisfied, which shows the existence of chaos. Our analysis using a Fractal map also implies that the system exhibits chaotic behavior when g^2/λ is not too much larger than unity. For larger g^2/λ, the backreaction of field fluctuations on sub-Hubble scales works earlier than the time at which the Toda-Brumer test is satisfied for the background field χ. We find signatures of chaos for $g^2/\lambda < \mathcal{O}(10)$ at the linear regime before the backreaction begins to work. For $g^2/\lambda \gg 1$ the quasi-homogeneous field χ gets smaller at the beginning of preheating, in which case perturbations enter a nonlinear region before chaos can be seen.

The system with a quadratic ($n = 2$) potential can not be effectively reduced to the analysis in Minkowski spacetime unlike the quartic potential. We first analyze the preheating dynamics in a frictionless background and then proceed to the case in which the expansion of universe is taken into account. In this model the background field χ does not grow sufficiently to satisfy the Toda-Brumer test in the presence of the backreaction effect of created particles. We find that this result holds both in Minkowski and expanding backgrounds. Therefore chaos can not be observed at least at the linear stage of preheating before the backreaction sets in.

When chaos is present, this means that the second field χ gives a non-negligible contribution for the background dynamics. This generally gives a strong correlation between adiabatic and isocurvature metric perturbations [38], which can lead to the amplification of curvature perturbations for the self-coupling inflation model [39]. This reduces the tensor to scalar ratio r, which is favorable from the observational point of view. Of course the ratio r is not sufficient to judge whether the model is rescued or not, since large contribution of isocurvature perturbations modifies the CMB power spectrum. It is still interesting that the appearance of chaos has a possibility to reduce the ratio r.

In this work we did not study the nonlinear dynamics of the system during which the mode-mode coupling between perturbations plays an important role. We expect that the presence of chaos persists even in such a nonlinear stage provided that two interacting fields ϕ and χ are dynamically important. The chaos would finally disappear after the energy densities of scalar fields are converted to that of radiation. It is of interest to extend our analysis to such a regime including Born decays of scalar fields for a complete understanding of chaos in reheating.

ACKNOWLEDGMENTS

It is a pleasure to thank Kei-ichi Maeda and Alexei Starobinsky for useful discussions. This work was partially supported by a Grant for The 21st Century COE Program (Holistic Research and Education Center for Physics Self-organization Systems) at Waseda University.

---

[1] A. Dolgov and A. Linde, Phys. Lett. **116B**, 329 (1982); L. Abbott, E. Farhi and M. Wise, Phys. Lett. **117B**, 29 (1982).

[2] J. H. Traschen and R. H. Brandenberger, Phys. Rev. D **42**, 2491 (1990); Y. Shtanov, J. H. Trashen and R. H. Brandenberger, Phys. Rev. D **51**, 5438 (1995).

[3] L. Kofman, A. D. Linde and A. A. Starobinsky, Phys. Rev. Lett. **73**, 3195 (1994) [arXiv:hep-th/9405187].

[4] D. Boyanovsky, H. J. de Vega, R. Holman, D. S. Lee and A. Singh, Phys. Rev. D **51**, 4419 (1995) [arXiv:hep-ph/9408214].

[5] E. W. Kolb, A. D. Linde and A. Riotto, Phys. Rev. Lett. **77**, 4290 (1996) [arXiv:hep-ph/9606260]; E. W. Kolb, A. Riotto and I. I. Tkachev, Phys. Lett. B **423**, 348 (1998) [arXiv:hep-ph/9801306].

[6] L. Kofman, A. D. Linde and A. A. Starobinsky, Phys. Rev. Lett. **76**, 1011 (1996) [arXiv:hep-th/9510119]; I. I. Tkachev, Phys. Lett. B **376**, 35 (1996) [arXiv:hep-th/9510146]; S. Khlebnikov, L. Kofman, A. D. Linde and I. Tkachev, Phys. Rev. Lett. **81**, 2012 (1998) [arXiv:hep-ph/9804425].

[7] H. Kodama and T. Hamazaki, Prog. Theor. Phys. **96**, 949 (1996) [arXiv:gr-qc/9608022]; A. Taruya and Y. Nambu, Phys. Lett. B **428**, 37 (1998) [arXiv:gr-qc/9709035]; B. A. Bassett, D. I. Kaiser and R. Maartens, Phys. Lett. B **455**, 84 (1999) [arXiv:hep-ph/9808404]; M. Parry and R. Easther, Phys. Rev. D **59**, 061301 (1999) [arXiv:hep-ph/9809574]; F. Finelli and R. H. Brandenberger, Phys. Rev. Lett. **82**, 1362 (1999) [arXiv:hep-ph/9809490]; B. A. Bassett, F. Tamburini, D. I. Kaiser and R. Maartens, Nucl. Phys. B **561**, 188 (1999) [arXiv:hep-ph/9901319]; S. Tsujikawa and B. A. Bassett, Phys. Lett. B **536**, 9 (2002) [arXiv:astro-ph/0204031].

[8] A. M. Green and K. A. Malik, Phys. Rev. D **64**, 021301 (2001) [arXiv:hep-ph/0008113]; B. A. Bassett and S. Tsujikawa, Phys. Rev. D **63**, 123503 (2001) [arXiv:hep-ph/0008328]; F. Finelli and S. Khlebnikov, Phys. Lett. B **504**, 309 (2001) [arXiv:hep-ph/0009093]; F. Finelli and S. Khlebnikov, Phys. Rev. D **65**, 043505 (2002) [arXiv:hep-ph/0107143]; T. Suyama, T. Tanaka, B. Bassett and H. Kudoh, Phys. Rev. D **71**, 063507

(2005) [arXiv:hep-ph/0410247].

[9] S. Y. Khlebnikov and I. I. Tkachev, Phys. Rev. Lett. **77**, 219 (1996) [arXiv:hep-ph/9603378]; S. Y. Khlebnikov and I. I. Tkachev, Phys. Rev. Lett. **79**, 1607 (1997) [arXiv:hep-ph/9610477].

[10] L. Kofman, A. D. Linde and A. A. Starobinsky, Phys. Rev. D **56**, 3258 (1997) [arXiv:hep-ph/9704452].

[11] P. Ivanov, Phys. Rev. D **61**, 023505 (2000) [arXiv:astro-ph/9906415]; K. Jedamzik and G. Sigl, Phys. Rev. D **61**, 023519 (2000) [arXiv:hep-ph/9906287]; S. Tsujikawa, JHEP **0007**, 024 (2000) [arXiv:hep-ph/0005105]; B. A. Bassett, M. Peloso, L. Sorbo and S. Tsujikawa, Nucl. Phys. B **622**, 393 (2002) [arXiv:hep-ph/0109176].

[12] B. A. Bassett and F. Viniegra, Phys. Rev. D **62**, 043507 (2000) [arXiv:hep-ph/9909353].

[13] F. Finelli and R. H. Brandenberger, Phys. Rev. D **62**, 083502 (2000).

[14] D. I. Podolsky and A. A. Starobinsky, Grav. Cosmol. Suppl. **8N1**, 13 (2002) [arXiv:astro-ph/0204327].

[15] M. Toda, Phys. Lett. A **48** (1974) 335.

[16] P. Brumer, J. Comp. Phys. **14** (1974) 391.

[17] G. L. Baker and J. P. Gollub, *chaotic dyansmics*: an introduction (Cambridge University Press, Cambridge, UK, 1996).

[18] J. D. Barrow and J. Levin, Phys. Rev. Lett. **80**, 656 (1998) [arXiv:gr-qc/9706065]; J. D. Barrow, Phys. Rept. **85** (1982) 1.

[19] R. Easther and K. i. Maeda, Class. Quant. Grav. **16**, 1637 (1999) [arXiv:gr-qc/9711035].

[20] J. Garcia-Bellido and A. D. Linde, Phys. Rev. D **57**, 6075 (1998) [arXiv:hep-ph/9711360].

[21] M. Bastero-Gil, S. F. King and J. Sanderson, Phys. Rev. D **60**, 103517 (1999) [arXiv:hep-ph/9904315].

[22] J. P. Zibin, arXiv:hep-ph/0108008.

[23] B. A. Bassett and F. Tamburini, Phys. Rev. Lett. **81**, 2630 (1998) [arXiv:hep-ph/9804453].

[24] N. J. Cornish and J. J. Levin, Phys. Rev. D **53**, 3022 (1996).

[25] S. E. Joras and V. H. Cardenas, Phys. Rev. D **67**, 043501 (2003) [arXiv:gr-qc/0108088].

[26] H. V. Peiris *et al.*, Astrophys. J. Suppl. **148**, 213 (2003); V. Barger, H. S. Lee, and D. Marfatia, Phys. Lett. B**565**, 33 (2003) [arXiv:hep-ph/0302150]; W. H. Kinney, E. W. Kolb, A. Melchiorri and A. Riotto, Phys. Rev. D **69**, 103516 (2004) [arXiv:hep-ph/0305130]; S. M. Leach and A. R. Liddle, Phys. Rev. D**68**, 123508 (2003) [arXiv:astro-ph/0306305]; S. Tsujikawa and A. R. Liddle, JCAP **0403**, 001 (2004) [arXiv:astro-ph/0312162]; S. Tsujikawa and B. Gumjudpai, Phys. Rev. D **69**, 123523 (2004) [arXiv:astro-ph/0402185].

[27] A. R. Liddle and S. M. Leach, Phys. Rev. D **68**, 103503 (2003) [arXiv:astro-ph/0305263].

[28] M. Tegmark *et al.* [SDSS Collaboration], Phys. Rev. D **69**, 103501 (2004) [arXiv:astro-ph/0310723].

[29] B. A. Bassett and S. Liberati, Phys. Rev. D **58**, 021302 (1998) [Erratum-ibid. D **60**, 049902 (1999)] [arXiv:hep-ph/9709417]; S. Tsujikawa, K. i. Maeda and T. Torii, Phys. Rev. D **60**, 063515 (1999) [arXiv:hep-ph/9901306]; *ibid*, Phys. Rev. D **60**, 123505 (1999) [arXiv:hep-ph/9906501]; *ibid*, Phys. Rev. D **61**, 103501 (2000) [arXiv:hep-ph/9910214]; S. Tsujikawa and H. Yajima, Phys. Rev. D **62**, 123512 (2000) [arXiv:hep-ph/0007351].

[30] A. R. Liddle and D. H. Lyth, *Cosmological inflation and large-scale structure*, Cambridge University Press (2000).

[31] D. I. Kaiser, Phys. Rev. D **53**, 1776 (1996) [arXiv:astro-ph/9507108].

[32] P. B. Greene, L. Kofman, A. D. Linde and A. A. Starobinsky, Phys. Rev. D **56**, 6175 (1997) [arXiv:hep-ph/9705347].

[33] J. P. Zibin, R. H. Brandenberger and D. Scott, Phys. Rev. D **63**, 043511 (2001) [arXiv:hep-ph/0007219].

[34] A. A. Starobinsky, in Field Theory, Quantum Gravity, and Strings, proceedings of the Seminar, Meudon and Paris, France, 1984-1985, edited by H. T. de Vega and N. Sanchez, Lecture Notes in Physics, Vol. 246 (Springer-Verlag, New York, 1986), p 107.

[35] K. i. Nakao, Y. Nambu and M. Sasaki, Prog. Theor. Phys. **80**, 1041 (1988).

[36] A. Hosoya, M. Morikawa and K. Nakayama, Int. J. Mod. Phys. A **4**, 2613 (1989).

[37] D. S. Salopek and J. R. Bond, Phys. Rev. D **43**, 1005 (1991).

[38] D. Langlois, Phys. Rev. D **59**, 123512 (1999) [arXiv:astro-ph/9906080]; C. Gordon, D. Wands, B. A. Bassett and R. Maartens, Phys. Rev. D **63**, 023506 (2001) [arXiv:astro-ph/0009131]; S. Tsujikawa, D. Parkinson and B. A. Bassett, Phys. Rev. D **67**, 083516 (2003) [arXiv:astro-ph/0210322].

[39] J. P. Zibin, R. H. Brandenberger and D. Scott, Phys. Rev. D **63**, 043511 (2001) [arXiv:hep-ph/0007219]; S. Tsujikawa, B. A. Bassett and F. Viniegra, JHEP **0008**, 19 (2000) [arXiv:hep-ph/0006354].